Flamelet Analysis of Turbulent Combustion

R.J.M. Bastiaans[1,2], S.M. Martin[1], H. Pitsch[1], J.A. van Oijen[2], and L.P.H. de Goey[2]

[1] Center for Turbulence Research , Stanford University, CA 94305, USA
[2] Eindhoven University of Technology, P.O.Box 513, 5600 MB Eindhoven, The Netherlands
r.j.m.bastiaans@tue.nl

Abstract. Three-dimensional direct numerical simulations are performed of turbulent combustion of initially spherical flame kernels. The chemistry is described by a progress variable which is attached to a flamelet library. The influence of flame stretch and curvature on the local mass burning rate is studied and compared to an analytical model. It is found that there is a good agreement between the simulations and the model. Then approximations to the model are evaluated.

1 Motivation and Objectives

The present research is concerned with the direct numerical simulation (DNS) and analysis of turbulent propagation of premixed flame kernels. The simulations are direct in the sense that the smallest scales of motion are fully resolved, while the chemical kinetics are solved in advance and parameterized in a table by the method of the flamelet generated manifolds (FGM) [8]. The state of the reactions are assumed to be directly linked to a single progress variable. The conservation equation for this progress variable is solved using DNS, with the unclosed terms coming from the table. This allows the use of detailed chemical kinetics without having to solve the individual species conservation equations.

Flame stretch is an important parameter that is recognized to have a determining effect on the burning velocity in premixed flames. In the past this effect has not been taken into account in the flamelet approach for turbulent combustion in a satisfying manner. The laminar burning velocity, which is largely affected by stretch, is an important parameter for modelling turbulent combustion. Flame stretch is also responsible for the creation of flame surface area, affecting the consumption rate as well. In the turbulent case, stretch rates vary significantly in space and time. An expression for the stretch rate is derived directly from its mass-based definition in [4],

$$K = \frac{1}{M}\frac{dM}{dt}, \tag{1}$$

where M is the amount of mass in an arbitrary control volume moving with the flame velocity:

V.S. Sunderam et al. (Eds.): ICCS 2005, LNCS 3516, pp. 64–71, 2005.

$$M = \int_{V(t)} \rho dV. \tag{2}$$

On the basis of this definition, a model for the influence of stretch and curvature on the mass burning rate has been developed. In a numerical study [5], it was shown that this model, with a slight reformulation, shows good agreement with calculations for spherically expanding laminar flames. This formulation, for the ratio of the actual mass burning rate at the inner layer, m_{in}, relative to the unperturbed mass burning rate at the inner layer, m^0_{in} (for unity Lewis numbers), reads

$$\frac{m_{\mathrm{in}}}{m^0_{\mathrm{in}}} = 1 - \mathcal{K}a_{\mathrm{in}}, \tag{3}$$

with the integral Karlovitz number being a function of flame stretch (1), flame surface area, σ, and a progress variable, $\mathcal{Y}$,

$$\mathcal{K}a_{\mathrm{in}} := \frac{1}{\sigma_{\mathrm{in}} m^0_{\mathrm{in}}} \left(\int_{s_u}^{s_b} \sigma \rho K \mathcal{Y} ds - \int_{s_{\mathrm{in}}}^{s_b} \sigma \rho K ds \right). \tag{4}$$

The integrals have to be taken over paths normal to the flame and s_u, s_b and s_{in} are the positions at the unburned side, the burned side and the inner layer, respectively. The flame surface area, σ, is related to the flame curvature, κ, which is related to the flame normals, n_i on the basis of the progress variable, $\mathcal{Y}$,

$$n_i = -\frac{\partial \mathcal{Y}/\partial x_i}{\sqrt{\partial \mathcal{Y}/\partial x_j \partial \mathcal{Y}/\partial x_j}}, \tag{5}$$

$$\kappa = \frac{\partial n_i}{\partial x_i} = -\frac{1}{\sigma}\frac{\partial \sigma}{\partial s}. \tag{6}$$

In turbulent premixed combustion the total fuel consumption is a result of the combined effect of flame surface increase and local modulation of the mass burning rate. In this study the latter will be investigated on the basis of (3) and possible parameterizations thereof, i.e. models for the Karlovitz integral, (4).

2 Methodology

Freely expanding flames are modelled in a turbulent flow field using DNS. More detailed information about the DNS program can be found in [1]. The fully compressible Navier-Stokes equations are solved supplemented by a conservation equation for the progress variable. For this purpose the mass fraction of carbon dioxide is used, which is monotonically increasing. Unity Lewis numbers are assumed for all species in order to prevent differential diffusion effects from obscuring the direct effects of stretch and curvature on the mass burning rate.

To make the DNS computations affordable, the FGM method of [8] is used to describe the reaction kinetics. FGM can be considered a combination of the flamelet approach and the intrinsic low-dimensional manifold (ILDM) method [7] and is similar to the Flame Prolongation of ILDM (FPI) introduced in [3]. FGM is applied similarly to ILDM. However, the thermo-chemical data-base is not generated by applying the usual steady-state relations, but by solving a set of 1D convection-diffusion-reaction equations describing the internal flamelet structure. The main advantage of FGM is that diffusion processes, which are important near the interface between the preheat zone and the reaction layer, are taken into account. This leads to a very accurate method for (partially) premixed flames that uses fewer controlling variables than ILDM. The manifold used in this paper is based on the GRI3.0 kinetic mechanism with 53 species and 325 reversible reactions [9].

The initial conditions are a laminar spherical flame superimposed on a turbulent field. There is no forcing in the simulation, so the turbulence will decay in time. The chemistry is chosen in relation to the large interest in the power industry in lean premixed combustion engines and there is detailed knowledge of its chemical kinetics. Therefore premixed combustion of a methane/air mixture is used, with an equivalence ratio of $\phi = 0.7$. The evolution of the initial laminar spherical flame kernel to the initial size in the DNS is calculated with detailed chemistry with the CHEM1D code [2].

3 Results

The first simulation, denoted C1, is a lean case with an equivalence ratio of $\phi = 0.7$, domain size of 12 mm, an initial flame kernel radius of approximately 2.9 mm, turbulent fluctuations of $u' = 0.4$ m/s and a turbulence length scale of ℓ_t=1.15 mm. In order to allow for very mild perturbations, initially we study the results at a time equal to 0.026τ, with $\tau = \ell_t/u' = 2.9ms$, taken from the start of the simulation. The time of growth of the laminar flame kernel to the initial DNS size was about 5 ms. The burning velocity of a flat unstretched flame with respect to the unburnt mixture is equal to $s_L^0 = 18.75$ cm/s and the corresponding mass burning rate is $m^0 = 0.213$ kg/m^{2}s. The progress variable is taken to be the carbon dioxide mass fraction, normalized with the maximum adiabatic value. At the left side of figure 1 is a cross section of the field. The contours of the progress variable are deformed only very mildly. It is observed that the scale of the vorticity patches are larger than the integral flame thickness. For this field the mass burning rate is analyzed as a reference case.

Additional analyses are performed in order to assess the basic model (4) under varying physical conditions. The test cases are listed in table 1. In case C2, the effect of grid resolution is investigated. It is assumed that the FGM method is valid in the flamelet regime if the progress variable is approximated with enough accuracy. Since all lengths scales of the gradients of primary

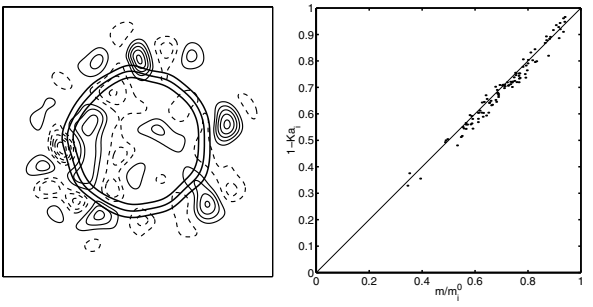

Fig. 1. Case C1, left: Vorticity contours (positive and negative values indicated by solid and dashed lines, respectively) and progress variable (thick lines, values 0.2, 0.5, 0.8), right: Correlation of the actual mass burning rate with the basic model (result of 52000 flamelets found in the domain)

Table 1. Physical properties correspondig to the different simulations

Case	ϕ	u' $[m/s]$	ℓ_t $[mm]$	δ_f $[mm]$	L $[mm]$	r_ini $[mm]$	grid	$\mathrm{Re_t} = \mathrm{u'}\ell_\mathrm{t}/\mathrm{s_L^0}\delta_\mathrm{f}$	tu'/ℓ_t
C1	0.7	0.40	1.15	0.614	12	2.9	254^3	4.0	0.026
C2	0.7	0.40	1.15	0.614	12	2.9	125^3	4.0	0.026
C3	1.0	0.60	0.89	0.475	12	2.9	254^3	4.0	0.026
C4	0.7	0.70	0.77	0.614	20	3.9	254^3	4.7	0.026
C5	0.7	1.31	0.94	0.614	12	2.9	254^3	10.7	0.026
C6	0.7	1.30	0.66	0.614	12	2.9	254^3	7.5	0.026

variables (i.e. the variables that are solved in the present DNS calcualations) are of the same order, this will yield satisfactory solutions. In order to assess the influence of the chemistry a stoichiometric case, C3, is selected, in which the same ratio of the turbulent velocity fluctuations compared to the laminar flame speed, and the turbulent integral length scale compared to the initial flame thickness as used for cases C1 and C2. For the stoichiometric case at unity Lewis numbers the burning velocity is $s_L^0 = 28.17$ cm/s and the corresponding mass burning rate is $m^0 = 0.316$ kg/m^{2}s. An additional case is given by the simulation of an increased initial flame kernel in a larger domain, C4. Here also the effective resolution is decreased. In addition, cases are chosen with increased velocity fluctuations and decreased length scales, cases C5 and C6, respectively.

In the analysis, the stretch rate defined by,

$$\rho K = \frac{\partial}{\partial x_i}(\rho s_L n_i), \tag{7}$$

is evaluated by using the relation for the local burning velocity s_L,

$$s_L = \left(\frac{\partial}{\partial x_i} \left(\frac{\lambda}{Le \bar{c}_p} \frac{\partial \mathcal{Y}}{\partial x_i} \right) + \dot{\rho} \right) \Big/ \left| \frac{\partial \mathcal{Y}}{\partial x_i} \right|, \tag{8}$$

which is a consequence of the combination of the conservation equation for $\mathcal{Y}$ with the kinematic equation for $\mathcal{Y}$. The latter defines the flame speed $u_{i\mathrm{f}}$ and then the relation for the flame velocity, $u_{i\mathrm{f}} = u_i + s_L n_i$, can be used to arrive at (8).

Table 2. Differences of the mass burning rate with the basic model

Case	C1	C2	C3	C4	C5	C6
Mean	0.0072	0.0081	0.0075	0.0091	0.0107	0.0094
RMS	0.0215	0.0202	0.0216	0.0236	0.0336	0.0280

Now the actual mass burning rate can be compared to model-values. This is performed by looking for points in the domain that are close to the inner layer and interpolate from there in the direction of positive and negative gradient of the progress variable, with steps of 1/20 times the gridsize. All relevant variables are interpolated over these flamelets and these flamelets are analysed to determine the burning velocity (8) and the model of the mass burning rate given by (4). For the present simulations these analyses lead to lots of starting points (e.g. for case C1: 52000) and thus resulting flamelets. For case C1 the correlation is depicted on the right side of figure 1. This shows that the model is a relatively accurate description of the actual mass burning rate. Deviations of the actual mass burning rate compared to the model (4) are given in table 2 for all six cases. It is seen that the mean error for all cases is about 0.01 or less, with a root mean square value of 0.02 to 0.03 (without normalization). It can be concluded that the model is a good description for all the present cases. Moreover, the grid coarsening shows no real deterioration, indicating that all cases are sufficiently resolved.

Starting from this point approximations to (4) can be considered. First, one can consider the case in which the surface area is taken to be constant, $\sigma = \sigma_{\mathrm{in}}$ as used frequently in the literature,

$$\mathcal{K}a'_{\mathrm{in}} := \frac{1}{m^0_{\mathrm{in}}} \left(\int_{s_u}^{s_b} \rho K \mathcal{Y} ds - \int_{s_{\mathrm{in}}}^{s_b} \rho K ds \right). \tag{9}$$

An improved model can be constructed by assuming that the curvature is not a function of the distance s, but that it remains constant equal to the inner layer value $\kappa = \kappa_{\mathrm{in}}$. By integrating (6) this yields for the surface

$$\sigma = \exp\left(-\kappa_{\mathrm{in}}(s - s_{\mathrm{in}})\right). \tag{10}$$

A third approximation is that the iso-planes of the progress variable are concentric, either cylindrical or spherical yielding

$$\sigma = \left(\frac{\xi/\kappa_{\mathrm{in}} - s}{\xi/\kappa_{\mathrm{in}}} \right)^{\xi}, \tag{11}$$

in which ξ takes the value 2 for spherical curvature and 1 for cylindrical curvature. This has to be limited for distances s beyond the concentric origin, $s > \xi/\kappa_{\text{in}}$, at which $\sigma = 0$.

Table 3. Differences of the mass burning rate determined by the basic model compared to the approximations

Case	C1	C2	C3	C4	C5	C6
$\sigma = \sigma_{\text{in}}$						
Mean	-0.0537	-0.0519	-0.0340	-0.0496	-0.0653	-0.0810
RMS	0.0552	0.0473	0.0373	0.0641	0.0772	0.1004
$\kappa = \kappa_{\text{in}}$						
Mean	0.0062	0.0055	0.0029	0.0026	0.0082	0.0079
RMS	0.0103	0.0085	0.0055	0.0173	0.0186	0.0338
$\xi = 2$						
Mean	-0.0011	-0.0006	-0.0007	-0.0075	-0.0037	-0.0141
RMS	0.0114	0.0101	0.0074	0.0313	0.0224	0.0540
$\xi = 1$						
Mean	-0.0059	-0.0050	-0.0032	-0.0115	-0.0101	-0.0219
RMS	0.0169	0.0142	0.0098	0.0333	0.0281	0.0556

The result of the approximations are given in table 3 for all cases. It is observed that the constant flame surface conjecture gives rise to relatively large error. There is a systematic over-prediction of about 0.05 (without normalization) of the mass burning rate with this model and the fluctuations are of the same order of magnitude. The other approximations give much better results. For the mean differences the spherical approximation, $\xi = 2$, is superior compared to the cylindrical model, $\xi = 1$, and for most cases also compared to the constant curvature model. However, this is not really substantiated when looking at the accompanying fluctuations. For the better resolved cases, C1 and C3, the mean difference is best predicted by the $\xi = 2$ model, but again the accompanying fluctuations are much larger than the model deviation. This suggests that it is not a real improvement. With respect to the fluctuations it seems that constant curvature gives the smallest deviations. Additionally, it can be observed that the constant curvature estimation gives slight under-predictions, whereas the concentric cases give systematic increased values of the mass burning rate. Moreover it can be seen that the stoichiometric case (C3) gives the smallest deviations for any of the present approximations. This indicates that the choice of progress variable for the lean case might not be the best choice.

For closer inspection of all realizations in the field, case C6 is chosen in which the deviations are largest. Correlation plots are shown in figure 2. For this case the basic model does not deviate significantly from the results in figure 1, the only difference being that the range of values is extended more to the origin of the plot. Moreover some features, as indicated above, are clearly reflected like

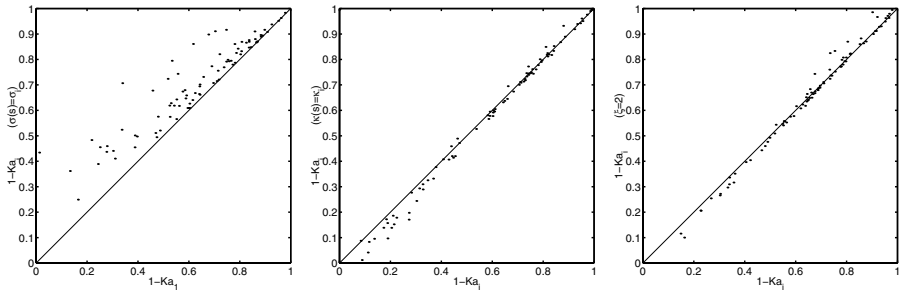

Fig. 2. Case C6, Correlation of the actual mass burning rate with the approximations, left: $\sigma = \sigma_{\text{in}}$, middle: $\kappa = \kappa_{\text{in}}$, right: $\xi = 2$, the case $\xi = 1$ deviates only very little from $\xi = 2$ and the figure is not given (result of 60000 flamelets found in the domain)

the under-prediction of the constant surface case. Furthermore the predictions of the concentric cases are less robust compared to the constant curvature model. The latter however gives deviations at small mass burning rates. This is also observed, to a lesser degree, in the concentric spherical approximation. Near the origin the cylindrical model seems to perform better. This is in agreement with observations in [6], who found that at higher turbulence levels, curvature in premixed turbulent combustion of flame kernels tends to cylindrical modes of deformation of the flame front.

It is obvious that all models do not fit to the true values because no local information on the flame geometry is taken into account in the approximations. If local geometric information is taken into account a much better agreement would be possible and will be a topic of further research. At larger times in the evolution, e.g. case C6, it was found that the basic model (4), gives good correlations (at $t = 0.087\tau$ mean deviation 0.08, rms values of 0.24), see figure 3, whereas all approximations are starting to deteriorate severely. In this case the curvatures have large values, the associated values of radii are within the flame thickness, δ_{f}, as shown in the figure (at the right).

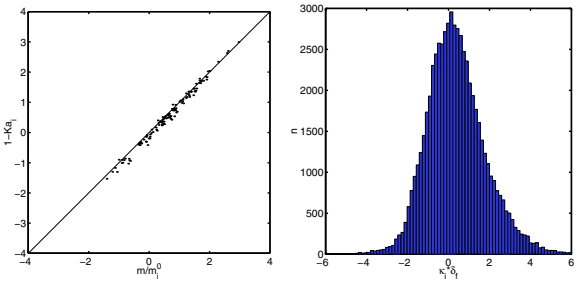

Fig. 3. Results of case C6 at time $t = 0.087\tau$, left: correlation of the actual mass burning rate with the basic model, right: PDF of inner layer curvatures

4 Conclusions

From the previous results it can be concluded that the method of FGM in combination with DNS calculations looks very encouraging. It appears that the FGM is a promising technique to reduce the chemistry and obtain accurate results for the flow, thermodynamics and species. However, apart from a validation in terms of laminar burning velocity, a direct validation is not present for turbulent cases. With respect to this, more validation is needed and the strategy for this will be twofold. By applying a suitable kinetics model with a limited number of species, a DNS can be conducted. This system can be reduced and validated directly against the results of the detailed chemistry calculations. A second method is to increase the dimension of the manifold. It must be studied how many controlling variables are required for a certain accuracy of the predictions. This again can be performed in the framework of the previously mentioned full chemistry DNS.

References

1. Bastiaans, R. J. M., van Oijen, J. A., Martin, S. M., de Goey, L. P. H. & Pitsch, H. 2004 DNS of lean premixed turbulent spherical flames with a flamelet generated manifold. In P. Moin, editor, *CTR Annual Research Briefs*, in press.
2. CHEM1D 2002 A one dimensional flame code. Eindhoven University of Technology, http://www.combustion.tue.nl/chem1d.
3. Gicquel, O., Darabiha, N. & Thevenin, D. 2000 Laminar premixed hydrogen/air counter flow flame simulations using flame propagation of ILDM with preferential diffusion. *Proc. Combust. Inst.* **28**, 1901-1908.
4. de Goey, L. P. H. & ten Thije Boonkkamp, J. H. M. 1999 A flamelet description of premixed laminar flames and the relation with flame stretch. *Comb. Flame*, **119**, 253-271.
5. Groot, G. R. A. & de Goey, L.P.H. 2002 A computational study of propagating spherical and cylindrical premixed flames. *Proc. Combust. Institute*, **29**, 1445-1451.
6. Jenkins, K.W. & Cant, R.S. 2002 Curvature effects on flame kernels in a turbulent environment. *Proc. Comb. Inst.*, **29**, 2023-2029.
7. Maas, U. & Pope, S. B. 1992 Simplifying Chemical Kinetics: Intrinsic Low-Dimensional Manifolds in Composition Space. *Combust. Flame* **88**, 239-264.
8. van Oijen, J.A. 2002 Flamelet-Generated Manifolds: Development and Application to Premixed Laminar Flames. Ph.D. thesis, Eindhoven University of Technology, The Netherlands.
9. Smith, G. P., Golden, D. M., Frenklach, M., Moriarty, N. W., Eiteneer, B., Goldenberg, M., Bowman, C.T., Hanson, R. K., Song, S., Gardiner Jr., W. C., Lissianski, V.V. & Z. Qin, Z. 1999 http://www.me.berkeley.edu/gri_mech/